

AD-A136 212

THE ROLE OF HYDROGEN IN THE STRESS CORROSION FAILURE OF  
HIGH STRENGTH AL... (U) IMPERIAL COLL OF SCIENCE AND  
TECHNOLOGY LONDON (ENGLAND) M L YUEN ET AL. OCT 83

1/1

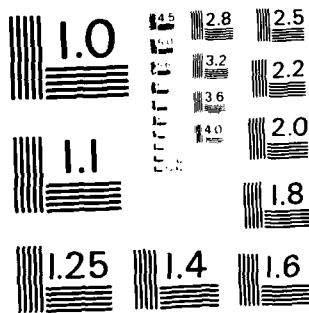
UNCLASSIFIED

DAJA37-80-C-0372

F/G 11/6

NL

END  
DATE  
FILMED  
1-84  
DTIC



MICROCOPY RESOLUTION TEST CHART  
NATIONAL BUREAU OF STANDARDS - 1963 - A

REPORT DOCUMENTATION PAGE		READ INSTRUCTIONS BEFORE COMPLETING FORM
1. REPORT NUMBER <b>ADA136 212</b>	2. GOVT ACCESSION NO.	3. RECIPIENT'S CATALOG NUMBER
4. TITLE (and Subtitle) The role of hydrogen in the stress corrosion failure of high strength Al-Zn-Mg alloys.		5. TYPE OF REPORT & PERIOD COVERED Annual Technical Report
7. AUTHOR(s) M. L. Yuen and H. M. Flower		6. PERFORMING ORG. REPORT NUMBER
9. PERFORMING ORGANIZATION NAME AND ADDRESS Imperial College of Science & Technology Prince Consort Road, London SW7 2BP		8. CONTRACT OR GRANT NUMBER(s) DAJA37-80-C-0372
11. CONTROLLING OFFICE NAME AND ADDRESS USARDSG-UK Box 65, FPO NY 09510		10. PROGRAM ELEMENT, PROJECT, TASK AREA & WORK UNIT NUMBERS
14. MONITORING AGENCY NAME & ADDRESS (if different from Controlling Office)		12. REPORT DATE Oct 83
		13. NUMBER OF PAGES
		15. SECURITY CLASS. (of this report) Unclassified
16. DISTRIBUTION STATEMENT (of this Report) Approved for public release; distribution unlimited.		15a. DECLASSIFICATION/DOWNGRADING SCHEDULE
17. DISTRIBUTION STATEMENT (of the abstract entered in Block 20, if different from Report)		Accession For NTIS GRA&I <input checked="" type="checkbox"/> DTIC TAB <input type="checkbox"/> Unannounced <input type="checkbox"/> Justification
18. SUPPLEMENTARY NOTES		By Distribution/ Availability Codes Avail and/or Dist Special <b>A7</b>
19. KEY WORDS (Continue on reverse side if necessary and identify by block number) Aluminium, dead load test, ductility ratio, fractography, hydrogen embrittlement, hydrogen trapping, life time, pre-exposure, scanning electron microscopy, slow strain rate.		
20. ABSTRACT (Continue on reverse side if necessary and identify by block number) Two alloys, Al 6% Zn 3% Mg 1.7% Cu and Al 6% Zn 3% Mg 0.14% Cr artificially aged at 120°C for times up to 400 hours have been tested at room temperature in tension in two aqueous environments, distilled water and 3.5% sodium chloride solution at strain rates of $10^{-4}$ s $^{-1}$ , $10^{-5}$ s $^{-1}$ , and $10^{-6}$ s $^{-1}$ . The results have been compared with previous data on fast and slow strain rate pre-exposure tests. Also conventional dead load tests were carried out in laboratory air and distilled water using the copper containing alloy. Both the slow strain rate technique and the dead load test are closely related and the		

DD FORM 1 JAN 73 1473 EDITION OF 1 NOV 65 IS OBSOLETE

Unclassified

SECURITY CLASSIFICATION OF THIS PAGE (When Data Entered)

DTIC FILE COPY

observations are consistent with the hydrogen model for embrittlement via reaction of the metal with the testing environment during straining or loading. The hydrogen adsorbed into the grain boundaries and the grain matrix causes grain boundary decohesion and cleavage. The ability to trap this hydrogen as innocuous hydrogen bubbles improves the embrittlement resistance. A peak embrittlement resistance is found to be around 150-250 hours of ageing at 120°C for the copper quaternary alloy. The embrittlement resistance mechanism and kinetics are not fully understood and may be complicated by the dissolution processes which accompany hydrogen generation. In this context the observation of grain boundary oxide films on the fracture surfaces of a small number of the dead load samples may be of importance.

## 1. INTRODUCTION

Previous studies (1) on the slow strain rate effect on the room temperature embrittlement of Al-Zn-Mg alloys exposed to water vapour at elevated temperature are consistent with the embrittlement model in which atomic hydrogen is injected into the metal during exposure and redistributed to the crack tip during testing. The transport of hydrogen is believed to occur via dislocation movement during plastic deformation (2-5). In some microstructures, trapping of hydrogen in the form of bubbles on the grain boundaries and the grain matrix (6,7) increases the tolerance of the metal to the total intake of hydrogen and thereby improves the embrittlement resistance (7). The results also demonstrate the importance of the intrinsic characteristics of the material and the local strain rate effect on the sample during testing. The embrittlement caused by the transport of atomic hydrogen via dislocations into the metal is a time dependent process. The lower the local strain rate and/or the more intrinsically ductile the metal is, the more time is allowed for such a dynamic embrittlement to take place. It is also observed that the faster the local strain rate and/or the more intrinsically brittle the metal is, the less dynamic embrittlement will affect the metal.

It is clearly important to establish whether the same basic process of hydrogen embrittlement also occurs under the conditions more typical of true stress corrosion. Therefore, the work has been extended to testing the same alloys in various aged conditions in distilled water and 3.5% aqueous sodium chloride solution over a strain rate range of  $4 \times 10^{-4} \text{ s}^{-1}$  to  $4 \times 10^{-6} \text{ s}^{-1}$  at room temperature. The purpose is to establish whether the embrittlement mechanism in an aggressive medium is still one of hydrogen embrittlement, as in the case of steam medium, or whether dissolution plays an important role. Additionally, conventional stress corrosion dead load tests have been performed on the copper quaternary

alloy in laboratory air and distilled water at room temperature.

The aim of the work is to determine whether the dead loading and slow strain rate tests are similar in providing ranking of materials in order of resistance to stress corrosion and hence whether the mechanism of cracking are truly similar in both cases. (8).

## 2. Experimental procedure

The chemical composition and the grain size of the two alloys studied are given in Fig. 1.

The preparation, heat treatment are similar to these described in the previous annual report (1).

### 2.1. Tensile tests

Tensile tests were performed at strain rates of  $4 \times 10^{-4} \text{ s}^{-1}$ ,  $4 \times 10^{-5} \text{ s}^{-1}$  and  $4 \times 10^{-6} \text{ s}^{-1}$  in distilled water and 3.5% sodium chloride aqueous solutions held in a perspex cell. Outside the gauge length, the specimen was protected with a lacquer (lacomit) to avoid galvanic corrosion. The specimen was removed from the environment immediately after failure. It was rinsed with distilled water and methanol, then stored dry in a dessicator prior to microscopic examination.

### 2.2. Dead load tests.

Conventional dead load tests were carried out in laboratory air and distilled water at a stress level of 20% above the estimated 0.2% proof stress of the corresponding heat treatment. The proof stress is obtained from the previous slow strain rate tests described in the annual report (1). The stress level was determined after initial experiments using loads both below and above the yield stress indicated that at lower stresses, the specimen life times would be impractically long. The sample was removed from the environment as soon as the failure was observed. The time elapsed between the failure and the removal of the sample ranged from one hour to two days. The samples were also rinsed with methanol and stored dry. Fig. 2 shows the set up of the dead load rig. (9).

### 2.3. Autoclave work

An autoclave (1) and a 3-point bending rig (Fig. 3), have been built to carry out stress corrosion tests in a steam environment at

elevated temperature. The object of this work is to study the relation between embrittlement with crack growth rate and the relation between crack growth rate with fracture toughness of this alloy. The 3-point bending test and the compliance method are adopted for this study because of the relative simplicity of the technique and the interpretation of the results. The compliance method requires a series of calibration tests. The 3-point bending sample of a notch depth  $a_0$  is elastically loaded in laboratory air, for instance in an Instron testing machine. The crack opening displacement, COD, is measured by a clip gauge and the load,  $P$ , is measured by a load cell built with a series of strain gauges. The compliance,  $C$ , the ratio of the crack opening displacement to the load is calculated:

$$C = \text{COD}/P$$

The relationship between the compliance and crack length is found by repeating this test on samples with different notch depths. The stress corrosion test involves loading up the specimen in the autoclave when the steam environment has reached the required temperature. The amount of load,  $P$ , applied is to give a stress intensity value  $K$  lower than the estimated critical value above which crack will propagate instantaneously. The relation is given as follows:

$$P = \frac{KBW}{6\sqrt{\pi a}}$$

where  $B$  = thickness of the sample

$W$  = width " " "

$a$  = crack length (notch depth + crack growth)

The specimen is left for the load to relax as the crack develops and grows. The load and the crack opening displacement are continuously measured using the load cell and the clip gauge. At any instant, the compliance can be derived and the crack growth can be obtained from the compliance  $V^S$  notch depth calibration. Knowing the crack length  $a$ ,

load,  $P$ , the stress intensity  $K$  can be calculated and the relation between the crack growth rate  $da/dt$  and the stress intensity factor can be derived.

The start of tests has been delayed owing to the difficulties encountered in building a load cell which would operate in the hostile steam environment under suitable protection. After preliminary trials, the assistance of the supplier of the strain gauges was sought to produce suitable cells to the required standard and reliability. At the time of submission of this report, the first tests are being undertaken.

#### 2.4. Fractography

The fracture surfaces were coated in 200 Å of gold and were examined in a scanning electron microscope. In selected cases, the matching fracture surfaces were mounted together so that fracture matching technique could be employed.

### 3. Results

#### 3.1. Copper quaternary alloy

##### 3.1.1. Tensile tests in aqueous environment.

In distilled water, the specimens underwent superficial corrosion and a large numbers of microcracks formed during loading. The presence of these led to considerable scatter in the apparent yield stress measurements but did not significantly affect fracture stress values (except for the slow strain rate saline environment tests). Since the fracture stress values were reproducible it is unlikely that the microcracks significantly affect the ductility values obtained which are presented in Figs. 4 a, b, for the distilled water environment and Figs. 5 a, b, for the saline environment. In both cases, ductility increases with increasing strain rate and increasing ageing time up to periods of the order of  $10^2$  hours at  $120^\circ\text{C}$ . The effect of the environment

is most obviously demonstrated by plotting the ratio of the observed ductility to that obtained in similarly aged material tested dry at the fastest strain rate (7) (i.e., conditions under which environment influence is minimal). The results are presented in Fig. 4b and 5b and indicate that gross overageing, although marginally increasing the absolute level of ductility, decreases the resistance to embrittlement in aqueous media. Figs. 4 and 5 also demonstrate the deleterious effect of salt which reduces the ductility ratio by a factor of approximately two for all aged conditions and strain rates examined.

As noted earlier fracture stress values were much less affected by environment and strain rate than was ductility. This is illustrated by Fig. 6 in which data for all tests, with the exception of the slow strain rate saline test, fall on the same curve as the fastest strain rate test in dry air.

Fractography of thin sheet tensile samples is necessarily complicated by the effect of a high surface to volume ratio in the sample and the varying local strain rate as a crack progresses through the sample. Therefore, as in previous discussion of fractography (1), the fracture is characterised by the topography of the regions adjacent to the crack initiation site where the strain rate is closest to the applied strain rate. In general the fracture faces were intergranular, the grain boundary facets exhibiting slip steps and networks of ductile dimples (plate 1). The fractographic characteristics are summarised in Fig. 7 together with test data from earlier (1,7) for comparison. Some corrosion of the fracture surfaces was observed but in general studies of matching fracture surfaces indicates that this is a post fracture phenomenon.

### 3.1.2. Dead load tests.

The samples were loaded to 20% above the estimated 0.2% proof stress.

Beyond 24-30 hours of ageing at 120°C, the material has reached the age hardening plateau which extends to over 400 hours ageing. Beyond 30 hours of ageing, the samples were, therefore, loaded to the same stress level. Solution treated material has a life in excess of 1100 hours when tested in air: life drops sharply with artificial ageing down to the plateau and then rises continuously with increasing ageing time (Fig. 8).

This behaviour contrasts sharply with that of samples tested in water where even in the solution treated condition, life is minimal and increases much more slowly with ageing. The life time ratio expressed as the ratio of the life time in air to that in water shows a maximum at approximately 120 hours ageing and a shape very similar to that of the ductility ratio data for the slowest strain rate shown in Fig. 4b. Since the fractographic data indicate that the slow strain rate samples failed post yield the dead load results may be taken as equivalent to ultra low strain rate data.

However, fractography is considerably more complicated than the above correspondence would imply. The fracture surfaces were in general intergranular throughout the fracture path and were brittle in appearance. A small number of samples exhibited life times well below the values shown in Fig. 8. In all such cases, the fractography indicated that premature failure had initiated at surface flaws which produce a notch effect. The fracture contained clear evidence of tensile overload containing coarse dimples and/or transgranular facets with quasi cleavage or micro-dimples. Additionally all samples exhibited a thick hydrated oxide layer about 1µm in thickness covering the entire fracture surface. In some cases when part of the oxide had decohered, fracture matching showed that the missing segments were present on the corresponding area of the other fracture surface (plate 2 a, b). This implies that at least part of the oxide film developed before the fracture crack opened up. Many micro-cracks were also observed. The fractographic studies are summarised

in Fig. 7. One dead load sample (copper containing variant in the solution treated condition) exposed to air for 1100 hours was deliberately overloaded to induce rapid fracture. Over 90% of the fracture surface was clearly formed during overload being ductile in nature. At one corner of the sample a small zone of brittle intergranular fracture was present. The fracture surface in this region was covered in a film which partially decohered from the surfaces and showed perfect matching on the two grain boundary surfaces (Plate 3 a, b). Clearly this oxide was present before the fracture crack opened up. The intergranular zone was surrounded by a narrow region of cleavage separating the ductile fracture from the intergranular regions. This zone is free of oxide and is presumably a hydrogen embrittled crack tip zone.

### 3.2. Chromium quaternary alloy

Tests have been performed on samples aged up to 70 hours at 120°C. There is no embrittlement when tested in distilled water at strain rates of  $4 \times 10^{-4} \text{ s}^{-1}$  and  $4 \times 10^{-5} \text{ s}^{-1}$  and in salt solution at  $4 \times 10^{-4} \text{ s}^{-1}$ . The ductility decreases as age hardening takes place and reaches a minimum value of about 7% after 40 hours ageing. At slower strain rates ductility is substantially reduced and is independent of the heat treatment condition. The ductility is plotted in Fig. 9a. The ratio of the ductility of this aqueous environment test to that of the fast strain rate dry sample (7) is plotted in Fig. 9b. Also included is the ratio of the ductility of the samples tested in air dried by silica gel at a strain rate of  $4 \times 10^{-4} \text{ s}^{-1}$  to that of the fast strain rate dry samples.

Although the ductility of the dry air, water ( $4 \times 10^{-5} \text{ s}^{-1}$ ) and salt solution ( $4 \times 10^{-4} \text{ s}^{-1}$ ) test results exhibit no significant reduction, the fractography shows evidence of embrittlement. All samples examined have a crack initiation region usually intergranular with multiple slip,

transgranular facets with dimples, cleavage and quasi cleavage.

The overloading region is always ductile intergranular often with a ductile shear tip along the edge. Fig. 10 summarises the fractographic observations. Also included are the results of the fast strain rate tests of the control samples (7).

#### 4. Discussion

The results of the slow strain rate and dead load tests are essentially similar in that they demonstrate the deleterious effects of decreasing strain rate in a chemically reactive environment and the increasing aggressiveness of air, distilled water and 3.5% salt solution. Dead loading can, therefore, in these test conditions be regarded as ultra low strain rate test. Given that the majority of the fractography is consistent with observations made in earlier work on pre-exposed material in which hydrogen is responsible for failure, the present results are consistent with the principal failure mechanism being one of the hydrogen embrittlement in all cases examined. Decreasing the strain rate increases the time available for the ingress of hydrogen into the metal and therefore increases the degree of embrittlement of otherwise ductile microstructures. Age hardening increases embrittlement resistance as grain boundary precipitates develop and form trap sites for hydrogen. The relative effects of the air, distilled water and salt solution can be rationalised by their effects on the breakdown of the initially protective oxide film on the metal and the subsequent generation of hydrogen at the metal surface. The role of chloride ions is well documented in this regard. The effects are further aggravated in the aqueous environments by the formation of surface pits which act as notches and hence, stress raisers. It should however be emphasised that in none of the tests carried out was any significant preferential dissolution of grain boundaries or other sites observed and the extent of corrosion pitting was small in relation to the specimen dimensions. In the aqueous tests the fractography implied that the fracture faces became oxide covered post fracture and that the active crack progressed through metal.

The presence of oxide on the fracture surfaces of the dead load samples tested in air and the matching of the oxide across the mating fracture faces seems initially surprising. However, the evidence

available does not imply, as suggested in other work (10), that the oxide forms along the grain boundaries prior to the passage of the crack. On the contrary, the deliberately overloaded air tested sample (plate 3 a, b) provides evidence only that the crack was filled with oxide prior to overload failure. If the small zone of intergranular fracture was caused by hydrogen penetration of the boundaries then a narrow crack would slowly grow into the metal which would have a hydrogen concentration profile in the boundaries and bulk of the metal ahead of the crack. The exposed boundaries are known to be highly reactive (1) and during the extremely long exposure time become covered in oxide which fills the narrow crack. Upon overload, this crack opens causing oxide to be torn and giving the observed matching on the fracture faces. The fast failure produces quasi cleavage in the hydrogen rich crack tip zone, as observed, and finally ductile failure of the environmentally unaffected metal.

The decrease in the ductility ratio and the life time of the material with increasingly aggressive test condition (lower strain rate and/or more hostile environment) can be explained by having more time available for corrosion and the breakdown of the passive film by the environment. However, it does not explain the different behaviour of the underaged material when tested in air from that tested in aqueous solutions. In air, the embrittlement resistance, e.g. indicated by the life time in the dead load tests, is initially high. The resistance drops sharply as age hardening occurs before it improves again when more hydrogen trap sites (grain boundary precipitates) are produced in the overaged condition. Similar samples tested in distilled water have no initial high life time but the life time also increases with ageing. The fractography gives no evidence of a different embrittlement mechanism operating in air from that in an aqueous solution and it offers no explanation for this anomalous observation.

Both the constant strain rate and dead load tests suggest the embrittlement resistance is improved with ageing, in agreement with most other studies on similar alloys (11,12). However, it was not expected that this copper quaternary alloy, when tested in aqueous environments, would exhibit a peak in the ductility ratio and life time ratio and a decreasing ratio with gross over ageing. Previous transmission electron microscopy studies (1,7) on this alloy show no substantial microstructural change except that the coarser and denser  $\eta$  phase ( $\text{MgZn}_2$  and  $\text{Mg}(\text{CuZn})_2$ ) precipitates on the grain boundaries and the coarsening of the  $\eta'$  phase in the grain matrix when the material is excessively overaged (beyond 300 hours at  $120^\circ\text{C}$ ). The  $\eta$  precipitates are known to act as hydrogen bubble nuclei (7) but they can also act as potential preferential anodic dissolution sites. Previous work on in-situ straining in the presence of water vapour (7) shows preferential attack on the grain boundaries and it is possible that in the aqueous media this contributes to the lower resistance compared with the air tests.

The addition of chromium to the alloy is believed to inhibit hydrogen entry (7). Previous slow strain rate tests show that when the passive film is continuously broken, the bare metal reacts with the moisture in air. Since this microstructure does not trap hydrogen readily, it is believed to be more vulnerable to dynamic embrittlement than the copper quaternary alloy. However, when samples aged up to 70 hours at  $120^\circ\text{C}$  were tested in aqueous environments at strain rate range of  $10^{-4}\text{s}^{-1}$  to  $10^{-6}\text{s}^{-1}$ , the chromium quaternary alloy showed no significant reduction in ductility unless the test aggressiveness was increased (Fig. 9a). The ductility ratio of these samples and the previous air samples (1) to that of the dry, fast strain rate samples presented in Fig. 9b indicates the relative embrittlement resistance of the alloy as the strain rate was reduced and/or as the environment became more hostile.

The ductility ratio of the aqueous samples increases with ageing (for those tests with ductility ratio below unity) while the ductility ratio of the samples slow strain rate tested in air (dried by silica gel) decreases with ageing for periods up to 70 hours at 120°C. In either air or the aqueous environments, the principal embrittlement mechanism is, again, consistent with the hydrogen model. At this stage of the research, no evidence has been observed to explain the different behaviour in air from that in aqueous solutions.

### Conclusions and proposals for further work

The extension of the work to aqueous environments and over a range of strain rate indicates that the transport of atomic hydrogen by dislocations is the principal embrittlement process. The dynamic embrittlement becomes more severe when the environment aggressiveness is increased (breakdown of the protective film) and/or when the overall strain rate is reduced (more time available for the injection and transport of hydrogen). The conventional dead load test is more time consuming than the slow strain rate technique but similar embrittlement resistance dependence with ageing is observed in both techniques. Therefore the slow strain rate test is a valid and more efficient technique to study stress corrosion cracking of a material in a relatively short period of time.

There are, however, a few observations that have not been explained: a peak embrittlement resistance at around 150-250 hours of ageing at 120°C and the different behaviour of the underaged microstructure when tested in air from that tested in aqueous solution. Further dead load tests of the materials in perfectly dry air or at stress level below proof stress may provide some explanation for these discrepancies. Gas chromatography technique can be used to obtain information on the production and injection of hydrogen in relation to the microstructure with the environment. Also the grain boundary chemical composition variation with ageing may also offer information on the dependence of embrittlement resistance with ageing. This will be performed using the scanning transmission electron microscopy and X-ray energy dispersive analysis on a thin foil. Special preparation of the thin foils eg. by ion beam thinning in ultra high vacuum is required to remove the copper and zinc rich surface oxide film present on electro-polished surfaces. Meanwhile the in situ stress corrosion work in a

steam environment held in an autoclave is to be continued and the results will be compared with the present observations.

## Reference

1. H.M. Flower, M.L. Yuen, U.S. Army Annual Report, European Research Office, Sept. 1982.
2. J.K. Tien, Proc. of the A.I.M.E. Conference on Effect of Hydrogen in Metals, Wyoming, 26-31 Aug. 1982. (edited by I.M. Bernstein and A.W. Thompson), 437, Aug. 1981.
3. J.A. Donovan, Met. Trans. 7A, 1677, Nov. 1976.
4. J.A. Donovan, Met. Trans. 7A, 145, Nov. 1976.
5. J. Albrecht, I.M. Bernstein and A.W. Thompson, Met. Trans. 8A, 811, May 1982.
6. S.V. Nair, R.R. Jensen and J.K. Tien, Met. Trans. 14A, 385, Mar. 1983.
7. L. Christodoulou, PhD Thesis, London University, 1980.
8. R.N. Parkins, A.S.T.M., Symposium on Stress Corrosion Cracking - The Slow Strain Rate Technique, Toronto, 2-4, May 1977, (edited by G.M. Ugiansky and J.H. Preyer), 5, Jan. 1979.
9. M.G. Lackey, PhD Thesis, London University, 1980.
10. C.O.S. Tuck and G.M. Scamans. Third International Congress on Hydrogen and Materials 7-11/VI/1982, Paris.
11. R.E. Swanson. Scr. Met. 16, 321, 1982.
12. G.M. Scamans  
Aluminium Dusseldorf 57 part 4, 268, 1981.

Alloy	Cr	Cu	Fe	Mg	Mn	Si	Ti	Zn	Balance Al	Grain size ( $\mu\text{m}$ )
Cu containig alloy(6/3 Cu)	0.001	1.7	0.02	3.0	0.001	0.01	0.01	6.3	"	30
Cr containing alloy(6/3 Cr)	0.14	0.003	0.01	2.99	-	0.02	-	6.11	"	25

Fig. 1. Chemical Compositions of the alloys (7)

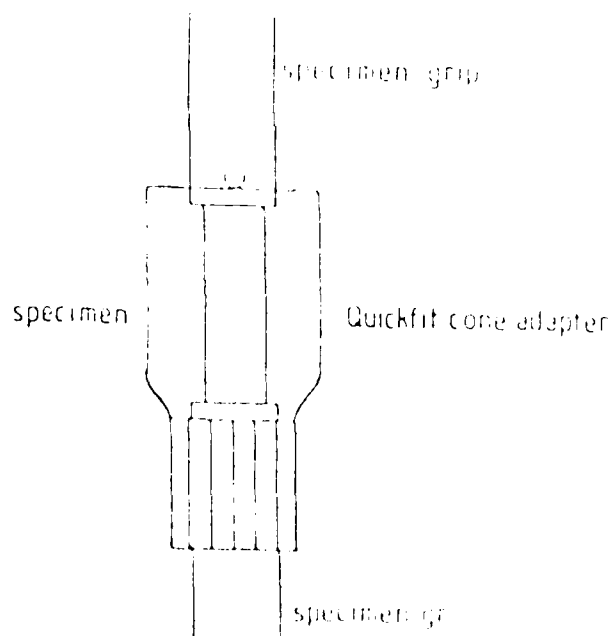


Fig. 2. Dead load rig.

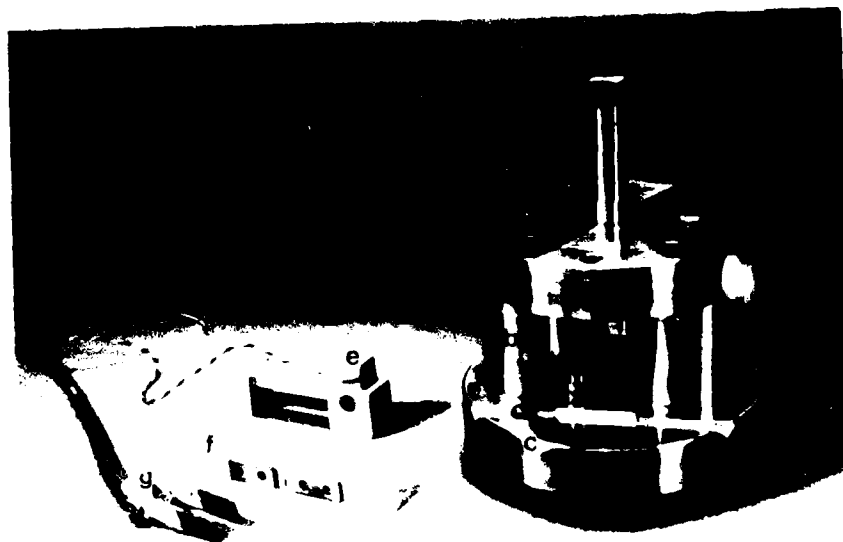


Fig. 3 - 4 point bending rig

a : top plate

b : spacers

c : bottom plate

e1 : grooves and ceramic rods to support the specimen

e2 : studs for positioning the specimen

d : bolt to apply a load on the specimen

g : load cell

f : a typical 4 point bending specimen with knife edges

g : cell output

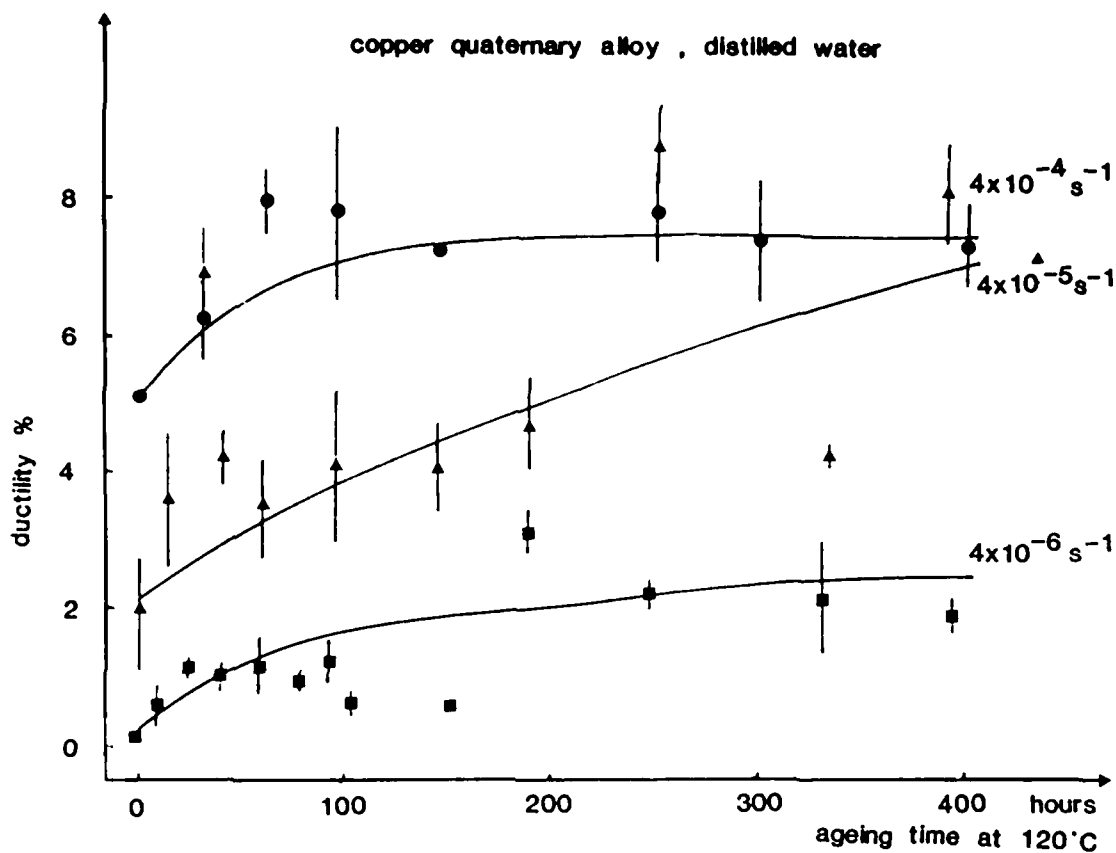


Fig.4a Variation of ductility with ageing time

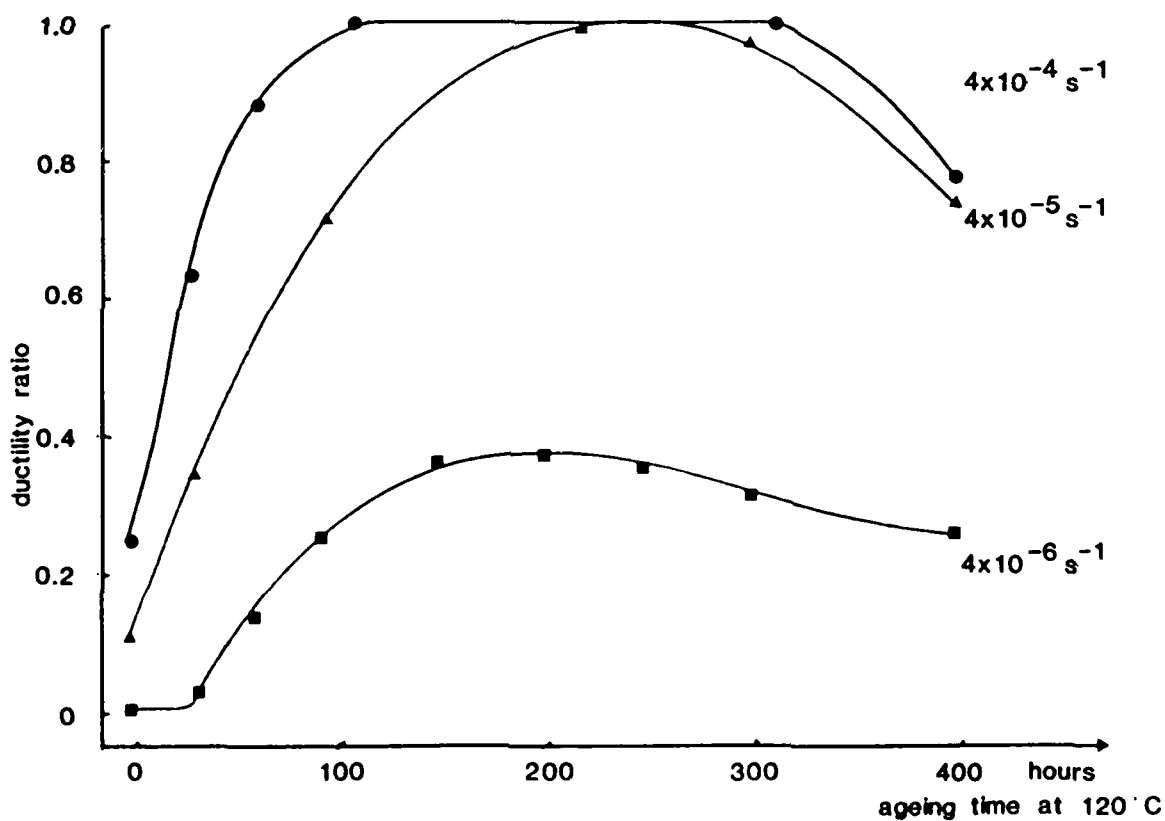


Fig.4b Variation of ductility ratio with ageing time  
Ductility ÷ ductility of fast strain rate dry samples

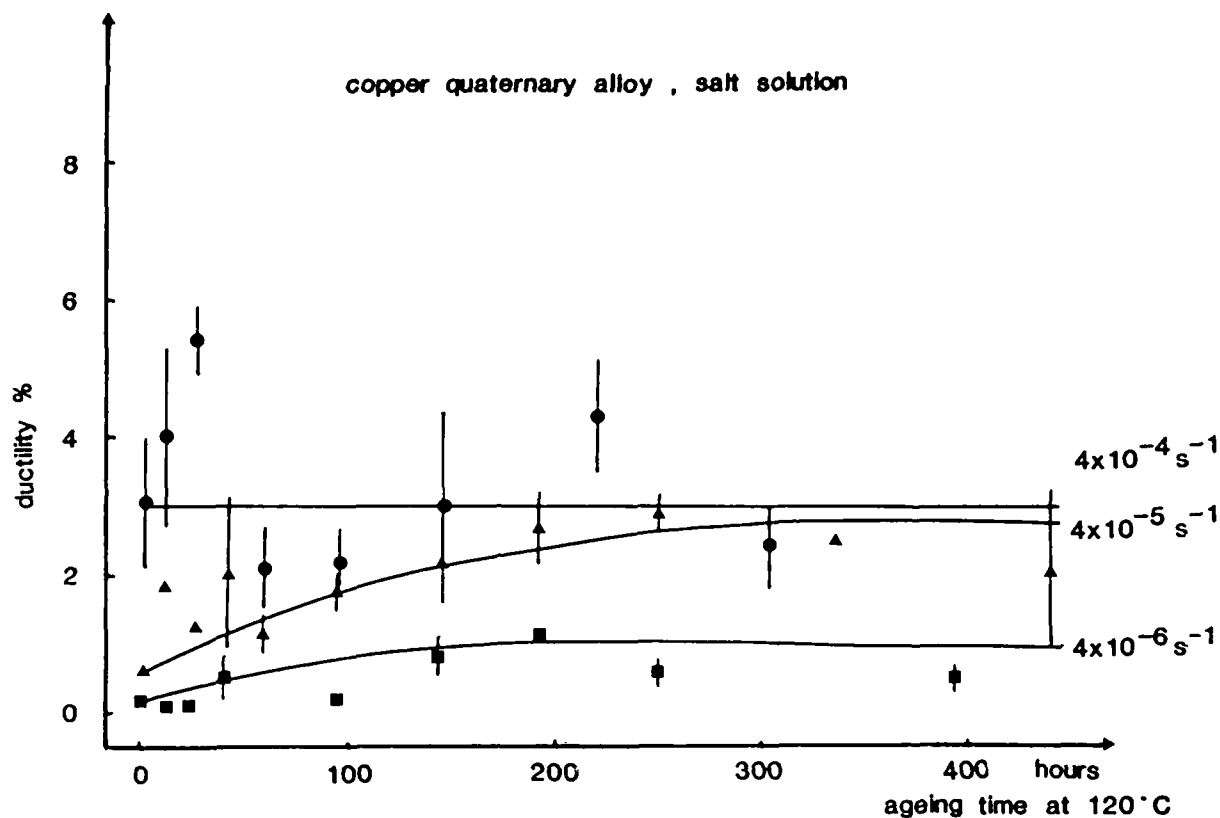


Fig. 5a Variation of ductility with ageing

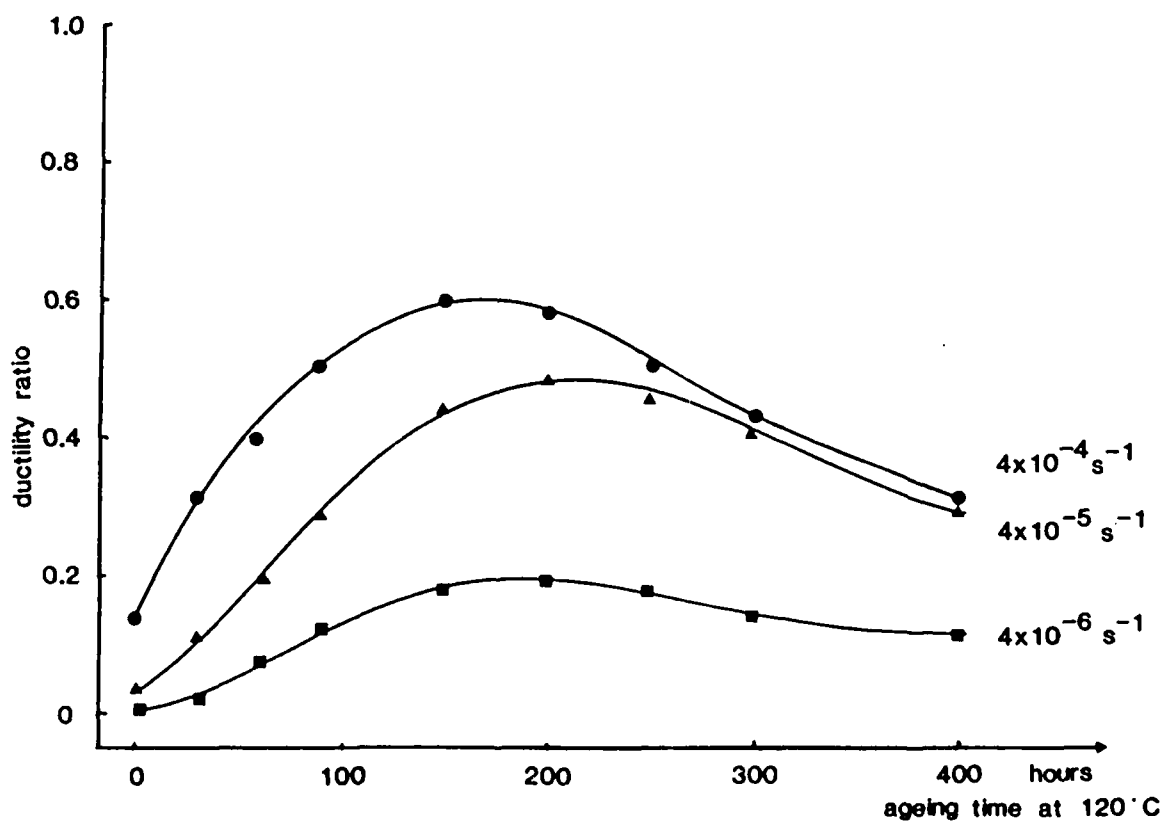


Fig. 5b Variation of ductility ratio with ageing  
Ductility + ductility of fast strain rate dry samples

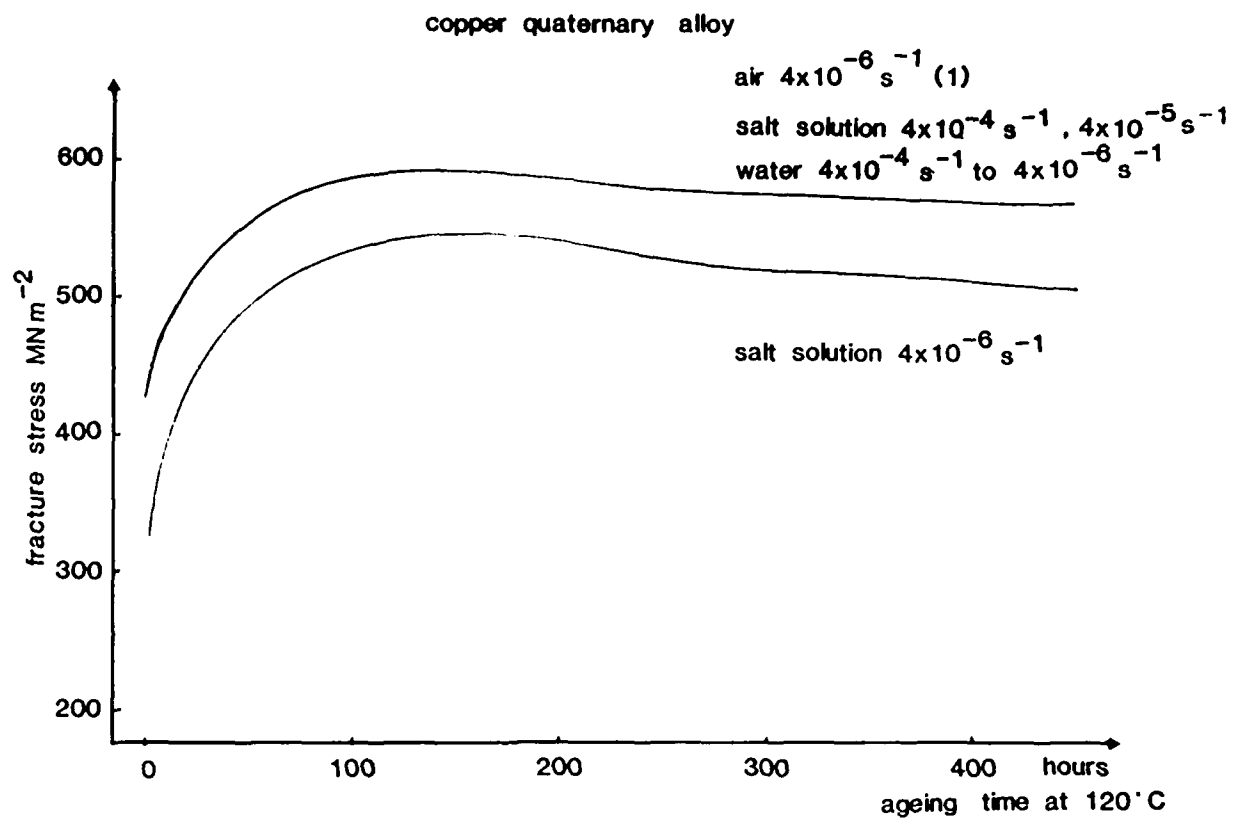


Fig.6 Variation of fracture stress with ageing  
(scatter  $\pm 10 \text{ MN m}^{-2}$ )

Environment	Strain Rate 4x - s <sup>-1</sup> or Dead Load	Ageing time at 120°C (Non uniform scale)									
		<div><div></div><div>0102030405060100200300400</div></div>									
Distilled water	10 <sup>-4</sup> 10 <sup>-5</sup>	IS, QC	IS, D 25% - 5%								
	10 <sup>-6</sup>	IS, QC	IS, D 20% - 10%								
Salt solution	10 <sup>-4</sup> 10 <sup>-5</sup>	IS	IS, D 8% - 2%								
	10 <sup>-6</sup>	IS						IS, D 5-2%			
Laboratory air	Dead Load	IS (QC, D ~ 2%)									
Distilled water	Dead Load	IS	IS, QC								
Pre-exposure in steam (1)	10 <sup>-6</sup>	IS, QC, D*	IS, D* 40-20%				IS, D 25-10%				
dry air (7)	10 <sup>-3</sup>	D						ID			

Fig. 7 Copper quaternary alloy -

Summary of fractographic observation

\* Fracture mode increasingly brittle towards the specimen surfaces

IS = intergranular + slip steps

ID = intergranular ductile

AC = quasi cleavage

D = transgranular dimples  
shown as %

C = cleavage

FT = flat transgranular with microdimples

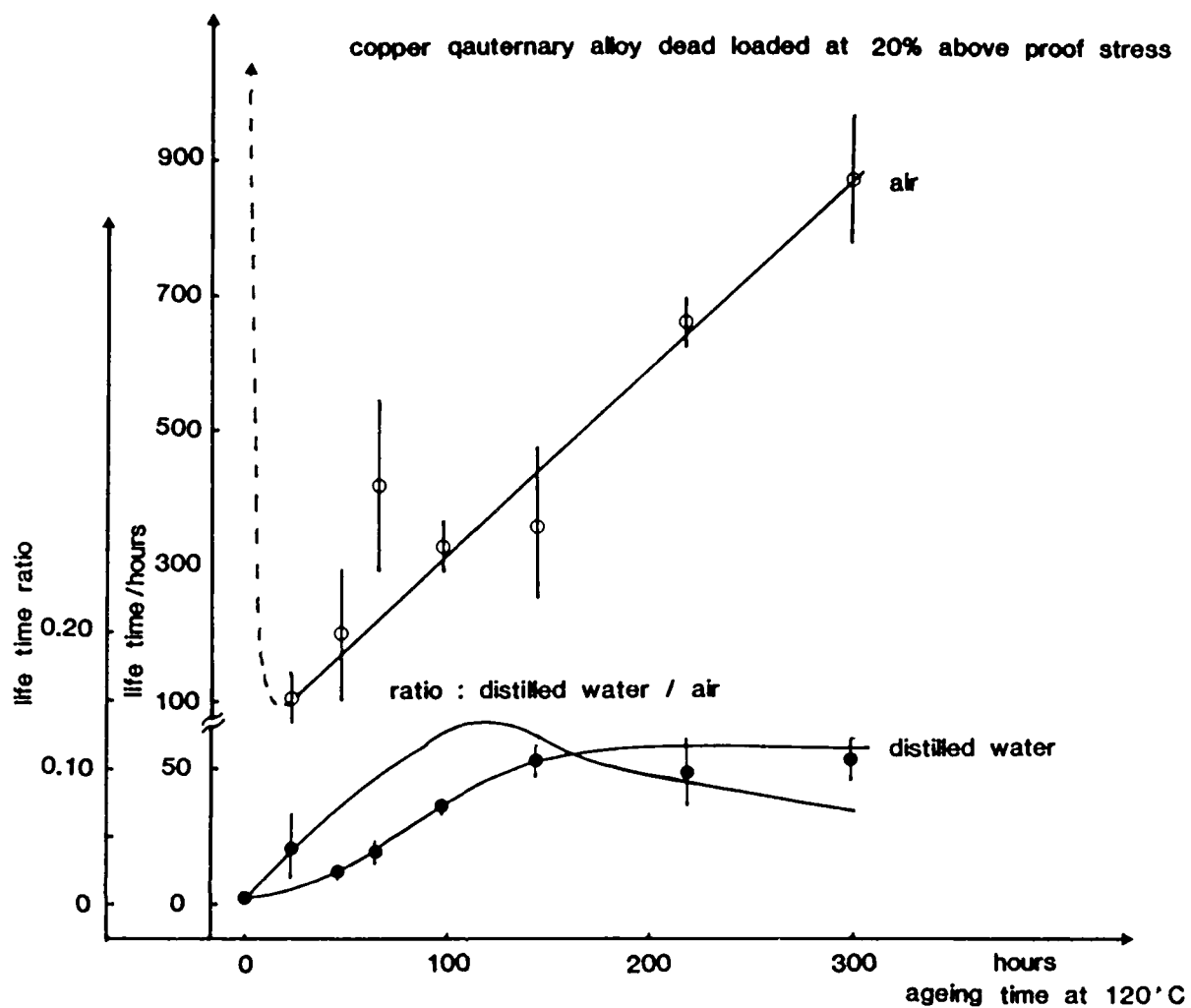


Fig. 8 Variation of life time and life time ratio with ageing

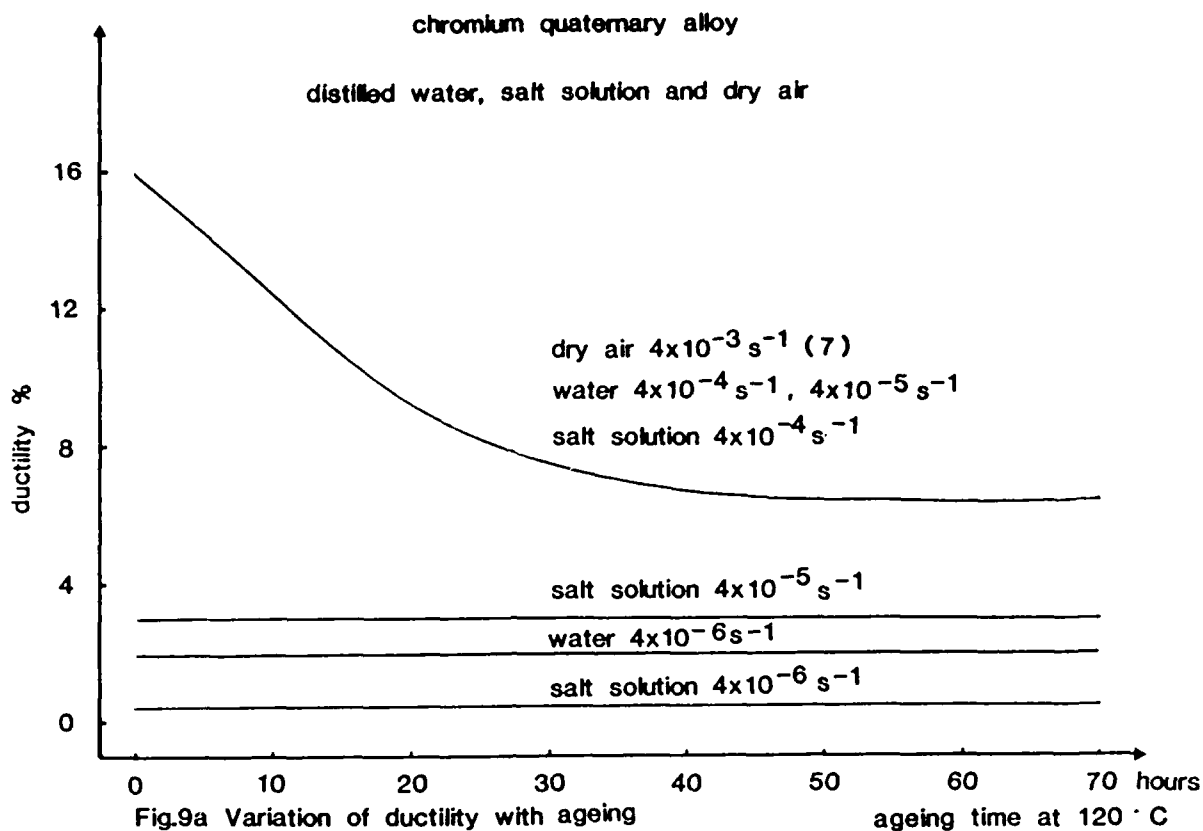


Fig.9a Variation of ductility with ageing

To avoid complication, experimental points are not shown.

The scatter is  $\pm 2\%$  for the high ductility curve and  
 $\pm 1\%$  for the lower ductility curves.

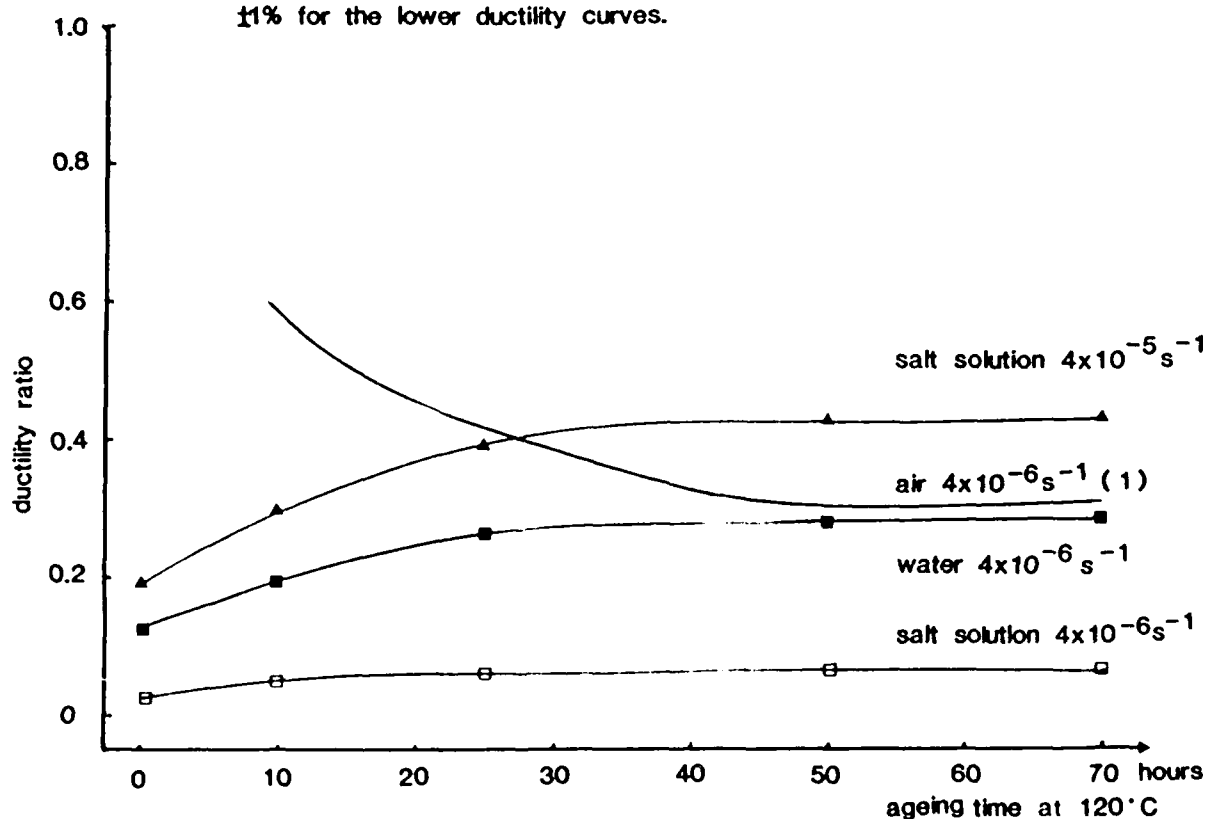


Fig. 9b Variation of ductility ratio with ageing

Ductility  $\div$  ductility of fast strain rate dry samples

Environment	Strain rate $4 \times 10^{-4} \text{ s}^{-1}$	Ageing time at 120°C			
		0	15	20	40
Distilled water	$10^{-4}$	FT	QC, FT*		
	$10^{-5}$	QC edge, FT, IS centre			
	$10^{-6}$	IS	Qc edge IS centre	IS, QC, FT	
Salt solution	$10^{-4}$	IS	IS, QC, FT*		
	$10^{-5}$	IS		IS, AC, C	IS, QC, C
	$10^{-6}$	IS, QC, C	IS, QC, C		
air dried by silica gel (1)	$10^{-6}$	ID, QC, D* ~60%	ID		
dry air (7)	$10^{-3}$	D			ID

Fig. 10 Chromium quaternary alloy

Summary of fractographic observation

For symbols, see Fig. 7.

Plate 1

Copper containing alloy, aged 24 hours at 120°C, tested in distilled water at a strain rate of  $4 \times 10^{-6} \text{ s}^{-1}$ , showing a typical intergranular fracture with networks of dimples.

Plate 2a, b.

Copper containing alloy, aged 144 hours at 120°C, dead loaded in distilled water, showing the matching of the oxide film on the grain boundaries of the mating fracture surfaces.

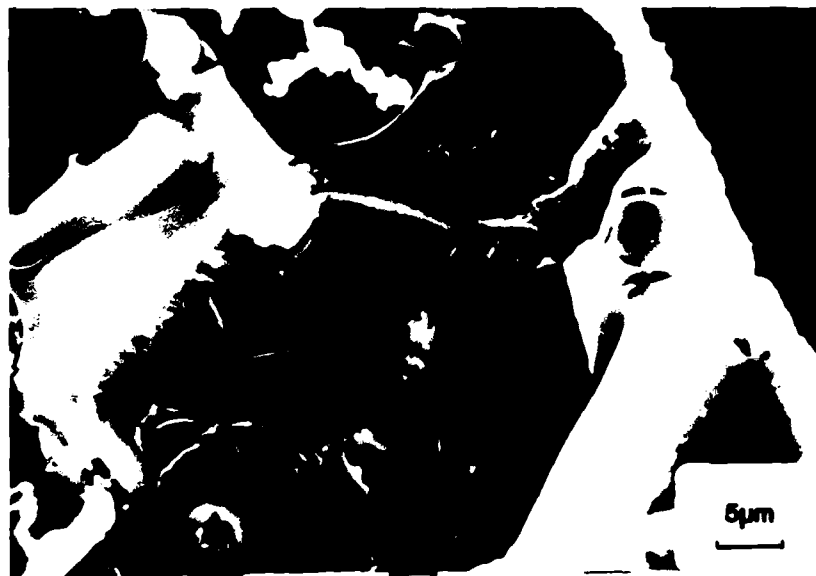
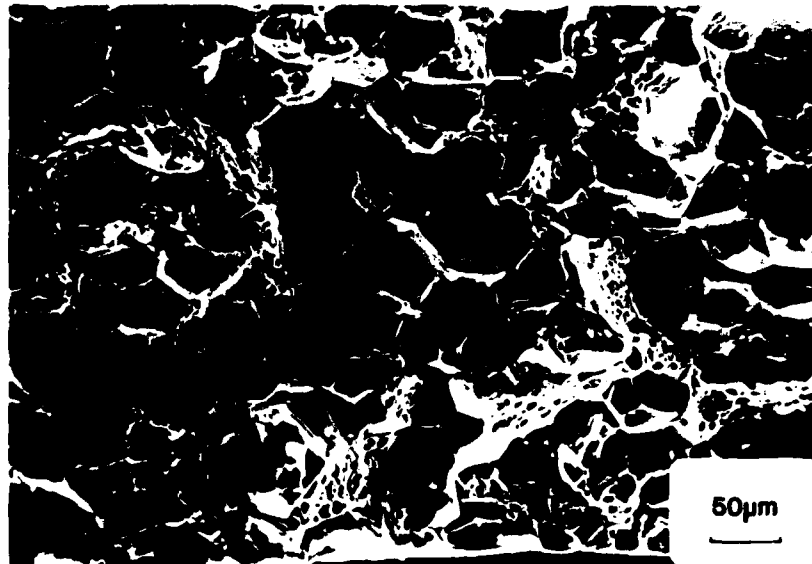


Plate 3 a, b.

Copper containing alloy, solution treated, overloaded after loading in air in excess of 1100 hours, showing the oxide film on the grain boundaries of the matching faces matches perfectly.

